Zeitschrift für Kristallographie, Bd. 138, S. 343—365 (1973)

The crystal structure of nuffieldite, $Pb_2Cu(Pb,Bi)Bi_2S_7$ *

By **Iwao Kohatsu** and **B. J. Wuensch**

Ceramics Division, Department of Metallurgy and Materials Science
Massachusetts Institute of Technology, Cambridge **

(Received 8 December 1972)

Auszug

Für die Struktur von Nuffieldit wurden die Raumgruppe *Pbnm* und die Gitterkonstanten $a = 14{,}387(7)$, $b = 21{,}011(15)$, $c = 4{,}046(6)$ Å, $\varrho_{\mathrm{gem}} = 7{,}01(7)$ g cm^{-3} und $\varrho_{\mathrm{x}} = 7{,}21$ g cm^{-3} bei $Z = 4$ gefunden. Für die Strukturbestimmung wurden die Intensitäten der Interferenzen in einer integrierenden Weissenberg-Kamera mittels der Äquiinklinations-Methode auf Mehrfachfilm aufgenommen. Die Struktur wurde nach dem Verfahren der symbolischen Addition ermittelt und mit der Methode der kleinsten Quadrate bis zu $R = 14{,}1\,\%$ verfeinert.

Die asymmetische Einheit enthält 13 Atome: fünf Schwermetallatome, ein Cu- und sieben S-Atome. Aus den Atomabständen und Koordinationen konnte für die Bi- und Pb-Atome je ein Paar von Atomlagen zugeordnet werden. Auf eine fünfte Lage sind beide Atomarten vermutlich statistisch verteilt. Der dominierende Bestandteil der Struktur ist eine vierfache $PbBiS_3$-Kette, die schon in dem einfacheren Sulfosalz Aikinit, $PbCuBiS_3$, gefunden worden ist, im Nuffieldit jedoch von einem Paar dreifacher $PbBiS_3$-Ketten flankiert wird, mit denen zusammen sie zehngliedrige Ketten bildet. Wie die viergliedrigen Ketten des Aikinits werden die zehngliedrigen Ketten an ihren beiden Enden durch Cu-Atome in tetraedrischer Koordination mit Nachbarketten zu Bändern verbunden.

Abstract

Nuffieldite, a rare bismuth sulfosalt from Alice Arm, British Columbia, is orthorhombic, space group *Pbnm*, with $a = 14.387(7)$, $b = 21.011(15)$, $c = 4.046(6)$ Å, $\varrho_{\mathrm{meas}} = 7.01(7)$ g cm^{-3} and $\varrho_{\mathrm{cal}} = 7.21$ g cm^{-3} for $Z = 4$. Intensity data were photographically recorded with an integrating equi-inclination Weissenberg camera employing the multiple-film technique, and were measured with the aid of an automated photoscanner. The structure was solved with the symbolic addition procedure and refined, by least-squares techniques, to a disagreement index of $14.1\,\%$. The asymmetric unit of the structure contains 13 atoms: 5 heavy-metal atoms, Cu, and seven S atoms. On the basis of interatomic distances and coordination geometry, Pb and Bi

---

* *Dedicated to Professor M. J. Buerger on the occasion of his 70th birthday.*

** Cambridge, Massachusetts 02139, U.S.A.

were each assigned to a pair of heavy-metal sites; a fifth site is believed to contain Pb and Bi in disorder. The Cu atom is in tetrahedral coordination. The dominant feature of the structure is a quadruple $PbBiS_3$ chain which is flanked by a pair of chains with Cu in tetrahedral coordination. This structural unit is identical to that found in the simpler sulfosalt aikinite, $PbCuBiS_3$. The aikinite-like ribbons share an edge with a pair of new three-membered chains to form ten-membered ribbons which are linked only by Cu tetrahedra and weak secondary bonds.

Introduction

Nuffieldite, a rare bismuth sulfosalt, was noted in the Lime Creek molybdenum deposit near Alice Arm, British Columbia, by DRUMMOND (unpublished) in 1960. A full description of these crystals, plus specimens from a nearby outcrop at Patsy Creek, was presented by KINGSTON (1968). The habit of crystals from the two sites differed. Those from Lime Creek were compact, small grains consisting of subparallel aggregates of stubby and deeply striated prisms. The crystals from Patsy Creek were prismatic to acicular, and were also deeply striated along the axis of elongation. X-ray examination (KINGSTON, 1968) showed both types of specimens to be the same mineral, although the lattice constants of the acicular crystals were slightly smaller.

Nuffieldite was found to be orthorhombic, with two moderately large lattice constants (14 and 21 Å). The third lattice constant, as is the case with virtually all known bismuth sulfides and sulfosalts, was equal to 4 Å. The ideal cell contents proposed by KINGSTON were $Pb_{10}Cu_4Bi_{10}S_{27}$. Although in good agreement with chemical analyses and the measured density, this composition is not compatible with the requirements of the possible space groups. The present structure determination was undertaken to clarify the composition of nuffieldite and, given the 4 Å lattice translation common to all members of this family, with the hope of revealing a structural relationship to simpler sulfosalts.

Material and x-ray examination

Crystals of nuffieldite were kindly supplied by Dr. KINGSTON. The samples consisted of one grain of the compact variety (which was not examined) plus the sole remaining crystals of the acicular type. The latter crystals were typically 1 mm in length and 0.01 to 0.03 mm in diameter. Most of the material supplied was found to be aikinite, $PbCuBiS_3$. Those needles identified as nuffieldite consisted, for the most part, of bundles of unterminated prisms having their axis of elongation in common, and were unsuitable for further work.

Only one crystal was found suitable for study and subsequent collection of intensities. It was a flat needle 0.3 mm in length. Careful measurement of its morphology revealed a triangular cross section with edges of 0.0180, 0.0165 and 0.0089 mm, which provided $\mu_l \, r_{\max}$ of 1.28 for Cu$K\alpha$ radiation ($\mu_l = 1423.9$ cm^{-1}). In view of the deep striations along the sides of the prism, this descripton of the shape must be regarded as only approximate.

Examination of the crystal with Weissenberg and Buerger precession techniques confirmed that nuffieldite is orthorhombic with $a = 14.45$, $b = 21.20$ and $c = 4.04$ Å. Systematic absences were observed in the diffraction patterns for reflections

$$\begin{array}{llll} h00 \text{ with } h \neq 2n & & h0l \text{ with } h + l \neq 2n \\ 0k0 \quad\quad\;\; k \neq 2n & & 0kl \quad\quad\quad\;\; k \neq 2n \\ 00l \quad\quad\;\;\; l \neq 2n & & \end{array}$$

The diffraction symbol is thus *mmm Pbn-*, which permits *Pbnm* (D_{2h}^{16}) or $Pbn2_1$ (D_{2v}^{9}) as possible space groups[1].

Table 1. *Lattice constants for nuffieldite*

	Present work acicular crystal[a]	Kingston (1968) acicular crystal	compact crystal[b]
a	14.387(7) Å	14.59(2) Å	14.602(6) Å
b	21.011(15)	21.21(2)	21.344(11)
c	4.046(6)	4.025(5)	4.026(2)
ϱ_{calc} [c]	7.170 g cm^{-3}	7.040 g cm^{-3}	6.989 g cm^{-3}
[d]	7.213	7.083	7.031
ϱ_{meas}	—	—	7.01(7) g cm^{-3}

[a] least-squares fit to 124 reflections.
[b] least-squares fit to 54 reflections.
[c] assuming cell content of $Pb_{10}Cu_4Bi_{10}S_{27}$.
[d] assuming cell content of $Pb_{10}Cu_4Bi_{10}S_{28}$.

---

[1] This is not in accord with the results of Kingston, who reported the same possible space groups, but in different settings (*Pnam* and $Pna2_1$). We suspect that an initial assignment of axes may have been changed to conform to the conventional labeling for cell edges, but that a corresponding transposition of the space-group symbol was inadvertantly omitted. Dr. J. D. Scott (Queen's University, Ontario) kindly provided Kingston's original Weissenberg photographs, and it was confirmed that they were identical to the patterns obtained in the present study.

Precise lattice constants were obtained through a least-squares fit to 108 *hk*0 and 16 *h*0*l* reflections recorded with a back-reflection Weissenberg camera. The systematic errors introduced by film shrinkage, sample eccentricity and absorption were accounted for with the aid of a program written by BURNHAM (1962). The results, Table 1, are in fairly good agreement with the lattice constants reported by KINGSTON.

Chemical composition

The very limited amount of material available for analysis presented problems in the establishment of a precise composition for nuffieldite. KINGSTON combined the results of a number of analytic techniques (x-ray spectroscopy, electron microprobe analysis, colorimetric analysis for sulfur, and atomic absorption analysis for the metals) to obtain 40.27% Pb, 5.88% Cu, 37.55% Bi and 16.30% S by weight. A measured density, 7.01(7) g cm^{-3}, could be obtained for only the compact material. Combined with the averaged chemical analyses, this provided empirical cell contents of $Pb_{10.22}Cu_{4.86}Bi_{9.45}S_{26.73}$, or an idealized composition of $Pb_{10}Cu_4Bi_{10}S_{27}$. The equipoints available in space groups *Pbnm* and *Pbn*2$_1$, however, have ranks of either 8 and 4, or 4, respectively. The Pb and Bi atoms therefore cannot be completely ordered. Moreover, unless some sites are only statistically occupied, the number of sulfur atoms per cell must be either 24 or 28. The latter possibility is closest to the results of the chemical analyses, but predicts a density which is high, Table 1, relative to that corresponding to the empirical formula. The compact grains of nuffieldite, however, being composed of an aggregate of subparallel prisms, might well contain voids which would provide an erroneously low measured density.

Intensity collection

Even the best crystal available consisted of two slightly misoriented domains which had their *c* axes in common. Weissenberg photographs obtained through rotation of the crystal about *c* thus displayed a slight splitting of reflections in ϕ. Intensities were therefore recorded with Ni-filtered Cu$K\alpha$ radiation with an integrating equi-inclination Weissenberg camera and the multiple-film technique. The range of the integrating motions (0.85 mm in Υ, 1.00 mm in ϕ) were selected to be large enough that both portions of the split reflections were incorporated in the integrated peak. Given the small value of the lattice constant c, the reflections were contained on but a few densely-populated levels in reciprocal space, and photographic methods proved in addition to be the most efficient means for recording the data.

The exposure time per level was forty integration cycles or approximately 140 hours. There were 1556 independent reflections within the Cu$K\alpha$ sphere of reflection. Of these, 1320 were accessible on the zero to third level of rotation about c. The fourth level ($\mu = 49°37'$) was mechanically inaccessible. The intensities were measured with an automatic photoscanner (Photoscan System P-1000, Optronics International, Inc., Chelmsford, Massachusetts) which produced a record of an optical density and two positional coordinates on a 100 × 100 micron raster on magnetic tape. The data were processed with a computer program written by one of us (I.K.) which displayed the density measurements around a desired reflection in a print-out. The difference between the plateau intensity of an integrated peak and background was extracted manually from the display.

Because of the large integration motion which it was necessary to employ, many weak reflections were indistinguishable from background in the displays. A minimum value was estimated for such intensities. These estimates were included in the final value of the reliability index, but not in subsequent analysis of the structure. Only 664 of the 1320 accessible reflections had intensity above the minimum detectable value.

The integrated intensities were corrected for Lorentz and polarization effects with the program FINTE (ONKEN, 1964). Corrections for absorption were performed with the program GNABS (BURNHAM, 1966) in which the crystal shape was approximated by five planar surfaces, and the numerical integration of the transmission factor was accomplished with an 8 × 8 × 8 grid based upon Gaussian quadrature. Because of the high linear absorption coefficient, and the approximate description of the crystal shape occasioned by the deep prism striations, the correction for absorption was the factor limiting both the accuracy of the final set of structure factors and the subsequent level of refinement of the structure.

Solution of the structure

Analysis of the structure was performed with the symbolic addition procedure. Normalized structure factors, E, were computed with the program FAME (FLEISCHER, DEWAR and STONE, 1967). The statistical

Table 2. *Statistical distribution of normalized structure factors*

	Computed value	Theoretical value	
		Centric	Acentric
$< E >$	0.808	0.798	0.886
$< E^2 >$	1.000	1.0	1.0
$< E^2 - 1 >$	1.052	0.968	0.736
Percent $E \geq 1.0$	28.22	32	37
Percent $E \geq 2.0$	5.77	5.0	1.80
Percent $E \geq 3.0$	0.47	0.3	0.01

distribution of E's, Table 2, suggested the centric space group *Pbnm* as the correct option, although this result was accepted with reservation inasmuch as scattering from the mineral is dominated by the heavy-metal atoms. Symbolic signs were assigned to a set of eight large (> 1.5) E's each of which displayed a minimum of 54 interactions. After ten iterations of the symbolic addition procedure with the program MAGIC (Fleischer *et al.*, 1967) the signs of 197 of 200 E's with magnitude greater than 1.0 were assigned. The sign group with minimum contradiction was then used to compute an E map. This clearly revealed the positions of five independent heavy atoms, all located in special position 4 *c m* of space group *Pbnm.* These positions were confirmed with a three-dimensional Patterson map. With Pb atoms and an arbitrary temperature factor of 1.0 Å^2 assigned to each metal site, the heavy-metal positions and scale factors for each of the four levels of data which were recorded were refined with the full-matrix least-squares program of Prewitt (1962). The reliability index, $R = \Sigma||F_{\text{obs}}| - |F_{\text{cal}}||/\Sigma\, |F_{\text{obs}}|$ converged to 24.6%. The scale factors remained within 10% of the preliminary values assigned on the basis of exposure time.

A Fourier map synthesized with structure-factor signs obtained on the basis of the heavy-atom positions revealed the locations of Cu and six sulfur atoms all in special position 4 *c m*. The sulfur atom locations provided only three S neighbors for the copper atom. This situation, although not without precedent in bismuth sulfides (*e.g.* Kupčik and Makovický, 1968; Ozawa and Takéuchi, 1972) is less usual than tetrahedral coordination. A weaker maxima appeared in the Fourier map at a location where an atom would be expected if the Cu coordination were to be four [S(1) in the description to follow]. Addition of this seventh sulfur atom to the asymmetric unit brought the sulfur-atom content of the cell to 28, in close accord with the chemical analysis. Subsequent refinement failed to provide evidence that this site was less than fully occupied. Upon the inclusion of the Cu atom and seven S atoms in the refinement, the disagreement index decreased to 18.1%.

Refinement of the structure

Upon examination of the agreement between F_{obs} and F_{cal} at $R = 18.1\%$, twenty-four structure factors were discovered to be grossly overestimated. These discrepancies were attributed to artifacts on the film. A similar situation had been encountered in analysis of another structure for which data had been obtained with an automatic photoscanner (KOHATSU and WUENSCH, 1973). Upon exclusion of these data from the refinement, R decreased to 16.8%. Bond lengths and angles were computed to permit assignment of Pb and Bi to the heavy-atom positions (as discussed below). Because of the close similarity of the scattering power of these atoms, distinction may be made only on the basis of relatively subtle differences in bond lengths and coordination. Upon identification of these atoms as Pb or Bi, corrections for anomalous scattering were applied for all atoms.

All reflections had been assigned equal weights in previous cycles of refinement. The weighting scheme adopted in subsequent cycles was taken as a function of $|F_{\text{obs}}|$ such that $[w(F_{\text{obs}}-F_{\text{cal}})^2]$ was constant for all values of F_{obs}. Under these conditions R decreased to 14.8%. The isotropic temperature factor for S(4) assumed a negative value and was fixed at a small magnitude, 0.01 Å^2, in subsequent cycles. Further refinement was attempted by the introduction of anisotropic thermal motion. Despite an increase in the number of parameters, no significant improvement in R (0.7%) resulted. Moreover, a difference map prepared upon convergence of isotropic refinement failed to provide decisive evidence for the need of anisotropic motion.

Refinement of an acentric model was attempted in view of the fact that the intensity statistics might be dominated by the heavy-atom distribution. Structurally, this relaxation permitted certain ribbon-like units of the structure to migrate along c relative to one another; in view of the small value of c, it was anticipated that such migration would be slight. It was found that no improvement in R obtained in the acentric model. More seriously, certain interatomic distances became unreasonable (*e.g.*, Cu—S 2.12 Å, and one heavy metal—S distance 2.42 Å). Similarly, in view of the problem of ac-

Table 3. *Atomic positions and temperature factors for nuffieldite*
(Estimated standard deviations enclosed in parenentheses; $z = 1/4$ for all atoms)

Atom	x	y	B
M(1) = Pb + Bi	0.1599(5)	0.1929(3)	0.90(11) Å^2
M(2) = Pb	0.3936(5)	0.3347(3)	0.88(11)
M(3) = Pb	0.6319(6)	0.0211(4)	2.04(15)
M(4) = Bi	0.6075(5)	0.4724(4)	1.14(12)
M(5) = Bi	0.9579(5)	0.3431(3)	0.99(11)
Cu	0.6691(18)	0.1722(11)	0.9(4)
S(1)	0.5417(48)	0.2399(30)	3.6(1.2)
S(2)	0.0169(34)	0.1117(21)	1.4(8)
S(3)	0.4718(24)	0.0676(17)	0.01[a]
S(4)	0.8026(26)	0.2276(16)	0.2(6)
S(5)	0.1438(31)	0.3724(20)	0.9(7)
S(6)	0.7417(44)	0.3883(28)	2.5(1.1)
S(7)	0.3190(28)	0.4687(19)	0.5(6)

[a] fixed.

comodating five Pb and five Bi in an ordered arrangement in space group *Pbnm*, refinement was attempted in several subgroups to take into account the fact that the crystal-chemical restraint that all heavy atoms lie close to $z = 1/4$ and $3/4$ might introduce false symmetry. Despite further increase in the number of adjustable parameters no improvement in R obtained and, again, unreasonable interatomic distances resulted.

The centric space group *Pbnm* was therefore adopted for the final refinement of the structure. Upon adjustment of scale factors, atomic positions, and isotropic temperature factors, refinement converged at 14.1% with a weighted R, $[\Sigma w(|F_{\text{obs}}| - |F_{\text{cal}}|)^2/\Sigma w F_{\text{obs}}^2]^{1/2}$ of 18.5%. Upon inclusion of the unobservable structure factors at $1/\sqrt{3}$ the estimated minimum observable value, the corresponding disagreement index and weighted R became 22.6% and 23.4% respectively[2]. The final atomic positions and isotropic temperature factors are presented in Table 3. The agreement between observed structure factors and those calculated from the parameters of Table 3 are presented in Table 4.

---

[2] The significant increase in R upon inclusion of the unobservable structure factors resulted from the fact that these values constitute a large fraction of the data (50%). Also, the experimental conditions which it proved necessary to employ produced a rather high value for the minimum detectable intensity.

Table 4. *Comparison of observed and calculated structure factors*
(Asterisk indicates unobservable structure factors estimated from one-third the minimum detectable intensity)

h	k	l	F_o	F_c
0	2	0	23.0*	25.1
	4		165.6	91.7
	6		735.2	975.1
	8		181.0	141.1
	10		175.9	159.2
	12		176.0	184.8
	14		383.6	382.5
	16		311.7	368.9
	18		78.4*	115.8
	20		206.7	229.6
	22		394.9	458.5
	24		118.8*	120.0
	26		54.0*	106.3
1	1	0	23.2*	16.5
	2		25.0*	9.2
	3		28.4*	19.7
	4		30.1*	30.2
	5		150.2	165.7
	6		37.9*	82.1
	7		191.3	181.7
	8		223.2	219.2
	9		48.1*	33.0
	10		51.5*	30.3
	11		145.0	119.3
	12		57.6*	142.2
	13		338.3	369.2
	14		329.4	340.2
	15		72.0*	84.5
	16		149.4	156.7
	17		76.2*	7.0
	18		77.0*	114.4
	19		79.7*	130.9
	20		177.3	188.6
	21		80.1*	8.7
	22		388.7	197.0
	23		73.8*	52.3
	24		128.6	183.6
	25		61.9*	17.2
	26		59.6*	98.3
2	0	0	227.4	200.3
	1		30.9*	72.4
	2		30.5*	24.2
	3		138.0	102.1
	4		215.0	192.3
	5		502.8	550.8
	6		140.9	125.8
	7		322.9	335.1
	8		45.9*	65.8
	9		177.9	149.0
	10		352.7	339.2
	11		790.8	854.8
	12		216.2	232.0
	13		161.4	182.2
	14		66.1*	87.1
	15		70.0*	35.2
	16		205.7	220.4
	17		493.6	560.3
	18		78.3*	132.5
	19		208.7	152.6
	20		79.7*	58.6
	21		78.7*	93.0
	22		145.1	209.3
	23		63.8*	116.3
	24		67.3*	58.3
	25		130.6	203.7
	26		51.8*	29.5
3	1	0	189.8	172.0
	2		35.4*	5.3
	3		437.1	481.7
	4		30.8*	129.6
	5		353.7	322.9
	6		188.3	149.0
	7		167.8	158.5
	8		48.1*	75.5
	9		308.5	305.9
	10		155.3	134.1
	11		57.6*	31.5
	12		60.8*	39.6
	13		64.4*	27.9
	14		68.0*	18.2
	15		71.2*	35.4
	16		171.9	125.4
	17		164.5	121.3
	18		79.0*	131.1
	19		80.3*	51.6
	20		80.1*	135.4
	21		78.9*	100.2
	22		76.0*	48.2
	23		211.9	201.6
	24		165.8	169.0
	25		199.6	196.1
	26		165.6	173.5
4	0	0	685.9	741.4
	1		586.2	496.8
	2		270.4	274.0
	3		42.2*	10.3
	4		417.6	403.9
	5		654.0	592.1
	6		661.2	628.6
	7		439.1	393.5
4	8	0	131.9	126.0
	9		284.8	226.7
	10		57.1*	97.2
	11		381.5	288.0
	12		63.8*	33.7
	13		67.3*	77.0
	14		262.2	311.7
	15		73.1*	4.8
	16		201.6	149.0
	17		78.0*	33.3
	18		232.6	278.0
	19		79.7*	11.3
	20		248.9	285.1
	21		221.3	217.2
	22		77.1*	145.8
	23		69.5*	63.9
	24		64.0*	35.0
	25		56.3*	19.8
	26		43.0*	136.8
5	1	0	225.3	219.4
	2		328.0	361.6
	3		190.4	174.5
	4		48.7*	100.6
	5		167.9	128.1
	6		161.7	242.9
	7		257.1	227.1
	8		502.9	477.3
	9		461.8	432.1
	10		60.8*	69.9
	11		64.2*	30.8
	12		152.2	155.1
	13		231.4	162.8
	14		374.3	449.8
	15		302.4	313.0
	16		78.1*	77.7
	17		79.4*	44.8
	18		80.3*	46.4
	19		80.1*	75.3
	20		302.3	347.8
	21		200.5	258.1
	22		77.1*	134.4
	23		67.2*	35.9
	24		61.1*	29.4
	25		51.8*	79.4
6	0	0	184.1	169.9
	1		203.8	186.7
	2		284.0	203.9
	3		237.6	237.4
	4		55.0*	38.9
	5		271.5	234.1
	6		57.2*	7.9
	7		348.6	410.5
	8		196.7	184.9
	9		448.3	404.9
	10		280.7	261.0
	11		294.3	292.1
	12		71.1*	128.7
	13		73.8*	135.1
	14		76.2*	19.4
	15		341.5	336.2
	16		279.7	288.2
	17		83.5*	158.5
	18		155.3	158.5
	19		80.8*	54.4
	20		77.0*	90.5
	21		75.4*	52.7
	22		125.5	102.0
	23		64.7*	31.6
	24		57.0*	130.4
	25		236.7	261.5
7	1	0	172.8	150.0
	2		390.5	410.3
	3		342.5	331.5
	4		484.3	524.3
	5		63.4*	8.7
	6		144.1	136.9
	7		195.6	154.3
	8		220.2	183.0
	9		147.2	112.9
	10		425.7	475.4
	11		72.5*	109.6
	12		74.8*	148.9
	13		77.2*	90.3
	14		79.1*	86.1
	15		82.3*	118.5
	16		82.1*	13.0
	17		82.1*	11.4
	18		81.5*	106.8
	19		79.9*	99.9
	20		224.2	265.6
	21		128.6	185.3
	22		140.9	152.5
	23		128.8	70.5
	24		35.9*	111.2
8	0	0	250.9	269.0
	1		314.7	288.3
	2		357.9	383.9
	3		257.1	250.6
	4		159.6	153.8
	5		160.8	179.0
8	6	0	170.0	152.5
	7		70.7*	77.3
	8		214.0	145.4
	9		330.2	328.8
	10		75.7*	68.1
	11		77.8*	78.0
	12		80.0*	55.6
	13		81.7*	61.2
	14		131.6	157.0
	15		275.6	259.8
	16		108.3	90.8
	17		82.5*	126.6
	18		80.5*	75.6
	19		78.0*	49.7
	20		198.7	201.9
	21		69.1*	35.1
	22		183.2	164.1
	23		54.3*	97.4
	24		41.6*	18.1
9	1	0	349.8	292.1
	2		250.1	246.1
	3		144.1	182.3
	4		329.1	290.0
	5		75.1*	12.6
	6		75.9*	90.8
	7		314.7	369.0
	8		78.9*	48.3
	9		303.4	306.2
	10		327.1	289.2
	11		83.5*	96.8
	12		166.6	182.6
	13		254.1	283.1
	14		86.9*	16.5
	15		432.9	474.5
	16		194.9	157.3
	17		83.4*	12.3
	18		80.1*	134.6
	19		75.7*	157.5
	20		70.4*	71.9
	21		335.2	344.1
	22		56.8*	47.1
	23		45.5*	44.8
10	0	0	85.0*	91.4
	1		225.2	226.1
	2		155.3	199.3
	3		190.3	156.5
	4		80.3*	138.6
	5		394.9	370.0
	6		81.4*	44.9
	7		82.7*	88.5
	8		84.1*	59.3
	9		343.5	339.5
	10		86.6*	111.5
	11		289.0	378.4
	12		88.3*	17.2
	13		88.4*	99.4
	14		136.0	132.9
	15		86.3*	109.3
	16		209.8	208.7
	17		80.9*	91.8
	18		76.6*	101.9
	19		71.3*	28.0
	20		180.0	239.9
	21		57.0*	87.6
	22		46.9*	4.9
11	1	0	482.3	421.5
	2		209.8	113.6
	3		51.4*	39.2
	4		308.6	381.5
	5		276.7	240.5
	6		86.1*	65.6
	7		249.9	272.1
	8		87.5*	107.5
	9		88.7*	124.3
	10		220.2	211.8
	11		89.5*	71.8
	12		89.0*	50.1
	13		88.3*	116.1
	14		86.5*	71.8
	15		203.6	230.5
	16		80.8*	45.7
	17		113.3	159.2
	18		71.3*	17.2
	19		65.1*	9.3
	20		57.4*	9.4
	21		146.3	190.2
12	0	0	253.0	193.2
	1		257.3	249.0
	2		193.3	176.0
	3		206.7	63.3
	4		88.4*	41.4
	5		259.2	192.0
	6		89.9*	128.3
	7		90.2*	107.7
	8		180.3	203.6
	9		89.9*	121.9
	10		284.8	283.2
	11		89.3*	155.9
	12		88.1*	157.7
	13		86.5*	21.2
12	14	0	85.3*	95.8
	15		79.9*	30.6
	16		238.6	298.3
	17		70.5*	15.7
	18		61.7*	85.2
	19		56.3*	105.7
	20		45.4*	72.7
13	1	0	83.4*	30.5
	2		84.5*	13.4
	3		222.2	220.5
	4		174.9	220.3
	5		89.9*	12.1
	6		203.7	193.0
	7		90.2*	68.6
	8		89.5*	53.8
	9		88.5*	29.0
	10		279.7	305.8
	11		85.4*	98.7
	12		214.1	231.3
	13		80.8*	10.4
	14		77.2*	85.9
	15		272.5	220.5
	16		188.4	199.3
	17		61.2*	23.6
	18		52.7*	135.7
	19		39.5*	101.6
14	0	0	332.2	423.0
	1		331.2	255.2
	2		80.0*	24.8
	3		81.0*	103.9
	4		82.1*	86.7
	5		306.4	191.6
	6		241.7	286.2
	7		82.7*	64.7
	8		82.3*	110.5
	9		162.8	169.3
	10		174.0	245.0
	11		77.8*	15.8
	12		154.8	190.1
	13		71.2*	36.7
	14		67.3*	122.4
	15		154.3	107.1
	16		257.7	272.6
	17		45.6*	34.3
15	1	0	211.9	234.1
	2		73.3*	22.8
	3		73.7*	90.6
	4		195.4	105.0
	5		281.4	243.1
	6		76.6	84.0
	7		72.9*	68.6
	8		71.7*	112.0
	9		70.4*	27.6
	10		68.0*	120.4
	11		64.7*	104.7
	12		61.6*	72.4
	13		211.2	245.8
	14		52.4*	91.8
	15		44.6*	49.2
16	0	0	64.4*	180.6
	1		64.6*	111.7
	3		64.6*	62.5
	4		202.6	117.6
	5		306.8	283.1
	6		62.6*	112.7
	7		104.1	44.8
	8		59.2*	188.4
	9		56.8*	76.0
	10		53.7*	2.5
	11		217.4	230.5
	12		45.0*	49.9
	13		37.7*	55.7
17	1	0	110.3	127.5
	2		153.3	117.6
	3		53.4*	27.2
	4		52.7*	6.0
	5		51.6*	9.6
	6		203.7	234.8
	7		162.5	75.8
	8		172.9	142.3
	9		41.2*	64.7
	10		180.2	191.8
18	0	0	190.3	184.3
	1		39.4*	83.0
	2		39.0*	80.5
	3		37.9*	58.3
	4		36.4*	14.5
	5		177.2	162.4
	6		206.0	222.1
0	2	1	281.7	282.5
	4		31.3*	18.5
	6		377.4	376.7
	8		580.0	636.9
	10		53.5*	48.5
	12		253.0	292.2
	14		411.4	434.0
	16		243.7	226.8
	18		316.8	365.1
	20		188.2	229.5
	22		390.8	333.2
0	24	1	154.4	169.6
	26		53.2*	101.8
1	0	1	106.4	137.8
	1		54.5*	75.7
	2		371.2	450.4
	3		165.6	170.3
	4		289.0	301.2
	5		460.7	460.0
	7		328.1	324.6
	8		358.9	354.4
	9		355.9	327.1
	10		53.3*	113.0
	11		177.0	159.8
	12		60.8*	10.9
	13		369.2	368.5
	14		68.4*	49.6
	15		128.6	120.9
	16		251.1	282.9
	17		77.9*	53.2
	18		79.9*	22.3
	19		204.9	222.7
	20		192.9	201.1
	21		157.7	161.7
	22		78.4*	93.1
	23		153.4	133.3
	24		141.8	124.9
	25		65.2*	81.6
	26		52.3*	109.7
2	1	1	384.6	330.9
	2		269.4	270.6
	3		515.2	618.5
	4		405.1	438.5
	5		468.9	500.5
	6		147.3	129.3
	7		204.7	184.6
	8		368.3	345.2
	9		372.3	360.7
	10		200.6	168.0
	11		380.5	382.6
	12		61.7*	22.7
	13		124.5	104.8
	14		217.1	221.7
	15		126.5	109.1
	16		75.3*	16.9
	17		77.8*	56.6
	18		79.7*	124.1
	19		165.6	156.7
	20		114.6	40.9
	21		80.0*	31.1
	22		77.4*	36.5
	23		73.8*	124.7
	24		69.7*	94.3
	25		136.4	139.9
	26		49.7*	83.1
3	0	1	229.3	227.1
	1		38.1*	53.9
	2		439.1	434.8
	3		387.7	360.0
	4		382.5	399.5
	5		122.4	113.9
	6		187.2	173.8
	7		351.7	368.6
	8		177.0	201.9
	9		531.7	559.3
	10		109.1	93.4
	11		66.8*	85.2
	12		143.1	126.8
	13		414.5	443.5
	14		70.1*	46.4
	15		304.5	339.1
	16		285.9	261.5
	17		297.3	308.6
	18		335.2	324.9
	19		193.5	204.3
	20		80.1*	49.4
	21		79.0*	66.9
	22		193.5	150.0
	23		206.7	238.5
	24		190.3	174.1
	25		139.9	60.8
	26		44.3*	7.6
4	1	1	135.8	102.5
	2		43.5*	35.5
	3		358.9	324.5
	4		160.8	144.3
	5		237.7	241.9
	6		46.3*	73.8
	7		231.6	251.0
	8		51.4*	96.0
	9		133.7	101.4
	10		58.0*	12.1
	11		225.3	163.7
	12		162.5	141.3
	13		406.2	452.4
	14		71.8*	108.5
	15		284.9	197.1
	16		253.1	213.5
	17		79.1*	89.3
	18		80.2*	12.3
	19		299.2	321.4

Table 4. *(Continued)*

h	k	l	F_o	F_c
4	20	1	79.7*	47.8
	21		78.3*	78.5
	22		228.4	288.0
	23		70.5*	62.1
	24		64.9*	18.8
	25		179.4	127.1
5	0	1	296.3	292.4
	1		406.2	383.0
	2		491.6	541.1
	3		49.9*	94.7
	4		389.7	353.0
	5		50.9*	27.8
	6		180.1	173.4
	7		469.9	471.4
	8		186.2	188.1
	9		212.0	284.1
	10		62.3*	61.9
	11		140.2	132.9
	12		68.6*	48.7
	13		320.8	354.9
	14		74.5*	40.6
	15		198.6	194.3
	17		80.8*	88.7
	18		81.5*	11.8
	19		80.8*	91.8
	20		245.8	286.2
	21		76.7*	34.1
	22		72.8*	22.4
	23		157.4	152.6
	24		61.6*	55.2
	25		51.2*	84.8
6	1	1	57.2*	8.3
	2		527.5	463.4
	3		56.9*	54.4
	4		340.4	293.5
	5		156.9	141.9
	6		324.9	308.6
	7		149.4	143.1
	8		241.7	205.3
	9		153.4	56.4
	10		66.7*	103.0
	11		216.0	201.7
	12		369.2	315.6
	13		75.2*	8.9
	14		78.0*	76.6
	15		60.4*	84.6
	16		82.2*	29.9
	17		149.7	175.0
	18		83.3*	71.0
	19		82.4*	52.8
	20		80.1*	36.1
	21		76.5*	33.5
	22		71.8*	29.7
	23		66.3*	55.8
	24		153.4	150.1
	25		39.2*	94.2
7	1	1	64.2*	85.0
	2		590.3	544.0
	3		62.8*	92.6
	4		533.7	482.7
	5		66.8*	134.0
	6		228.3	215.3
	7		67.8*	109.9
	8		67.3*	56.1
	9		282.8	280.2
	10		387.7	424.0
	11		74.6*	67.3
	12		515.2	538.8
	13		163.5	162.1
	14		184.1	161.8
	15		242.7	260.8
	16		82.0*	179.7
	17		83.7*	86.3
	18		446.3	515.3
	19		139.2	152.3
	20		132.0	127.2
	21		70.7*	14.5
	22		64.2*	14.3
	23		56.2*	17.1
	24		268.6	289.9
8	1	1	416.6	333.2
	2		66.7*	86.3
	3		67.5*	53.9
	4		188.4	155.6
	5		337.3	372.1
	6		71.6*	33.0
	7		73.0*	37.5
	8		74.3*	62.6
	9		76.3*	41.4
	10		205.8	94.3
	11		80.1*	32.0
	12		81.9*	4.2
	13		205.8	212.2
	14		84.9*	50.6
	15		87.1*	73.1
	16		113.1	161.7
	17		227.3	233.0
	18		82.1*	41.7
	19		126.6	137.8
	20		75.0*	60.3
8	21	1	69.4*	85.4
	22		62.0*	117.0
	23		253.0	279.8
9	1	1	507.0	437.3
	2		71.2*	119.1
	3		71.9*	81.8
	4		72.8*	17.8
	5		184.2	163.0
	6		206.9	260.2
	7		492.6	541.5
	8		78.4*	109.5
	9		180.0	133.4
	10		212.9	152.5
	11		82.9*	66.1
	12		195.4	174.0
	13		313.7	253.3
	14		85.6*	33.7
	15		148.6	151.6
	16		195.4	242.3
	17		81.7*	5.3
	18		78.8*	40.8
	19		74.4*	40.0
	20		69.3*	22.0
	21		62.4*	119.8
	22		128.8	159.7
10	1	1	78.2*	34.7
	2		133.8	132.1
	3		78.0*	11.6
	4		78.0*	39.0
	5		78.5*	23.1
	6		353.8	413.6
	7		130.6	222.2
	8		213.9	217.9
	9		82.9*	12.2
	10		84.0*	10.7
	11		85.4*	33.8
	12		313.7	381.9
	13		226.5	225.8
	14		86.1*	41.5
	15		146.9	146.3
	16		82.2*	64.5
	17		79.0*	7.6
	18		74.8*	110.1
	19		245.9	153.4
	20		62.5*	76.8
	21		53.7*	95.3
	22		38.6*	67.3
11	1	1	165.3	205.5
	2		80.6*	85.0
	3		81.0*	50.1
	4		293.1	311.3
	5		267.4	316.6
	7		158.4	196.3
	8		83.8*	7.1
	9		84.1*	76.2
	10		84.1*	157.2
	11		233.5	258.4
	12		225.2	265.0
	13		82.3*	52.1
	14		80.3*	50.7
	15		77.4*	55.0
	16		73.6*	5.4
	17		154.6	221.4
	18		255.0	381.0
	19		57.1*	26.4
	20		41.1*	9.3
12	1	1	263.2	125.0
	2		258.1	268.3
	3		303.4	312.9
	4		336.3	375.3
	5		308.6	187.5
	6		91.8*	16.7
	7		92.9*	115.7
	8		173.8	138.8
	9		173.8	130.5
	10		190.2	266.3
	11		93.1*	48.3
	12		91.7*	7.2
	13		160.6	142.4
	14		87.0*	31.7
	15		83.2*	76.3
	16		78.4*	34.2
	17		166.6	183.4
	18		110.0	140.6
	19		188.2	225.9
13	1	1	81.4*	124.7
	2		82.6*	53.4
	3		83.9*	29.8
	4		85.9*	9.2
	5		104.0*	137.6
	6		145.1	156.0
	7		253.2	253.0
	8		87.8*	73.9
	9		86.8*	36.2
	10		85.0*	1.5
	11		240.8	239.4
	12		103.9	108.0
	13		77.8*	124.8
	14		74.2*	8.6
	15		69.6*	95.9
13	16	1	63.8*	32.6
	17		160.7	193.5
	18		45.5*	36.9
14	1	1	76.1*	71.2
	2		246.8	276.8
	3		245.8	193.8
	4		78.7*	74.9
	5		79.0*	93.2
	6		131.9	135.0
	7		178.4	185.2
	8		407.2	423.8
	9		77.8*	33.6
	10		76.2*	62.8
	11		124.4	98.7
	12		70.2*	121.4
	13		156.4	165.4
	14		305.5	336.8
	15		55.7*	92.1
	16		47.2*	22.3
15	1	1	69.5*	16.8
	2		70.1*	6.1
	3		70.0*	58.0
	4		69.9*	8.9
	5		69.9*	43.0
	6		69.5*	75.0
	7		68.4*	28.6
	8		67.0*	8.1
	9		65.3*	80.0
	10		62.9*	28.5
	11		60.2*	103.3
	12		56.3*	69.8
	13		52.2*	55.1
	14		44.4*	17.6
16	1	1	60.6*	5.4
	2		60.7*	5.0
	3		421.5	459.8
	4		128.6	53.1
	5		59.2*	55.9
	6		57.9*	72.9
	7		172.8	47.1
	8		225.2	172.3
	9		169.8	251.1
	10		48.1*	99.4
	11		43.6*	61.6
	12		125.4	74.6
17	1	1	127.6	138.1
	2		131.3	129.7
	3		48.1*	18.2
	4		47.1*	55.0
	5		45.9*	54.4
	6		50.4*	48.6
	7		41.7*	119.1
	8		136.8	125.4
	9		31.8*	91.2
18	1	1	38.0*	12.8
0	2	2	27.5*	11.4
	4		36.4*	62.4
	6		674.5	782.1
	8		128.9	135.6
	10		148.1	133.3
	12		150.0	153.7
	14		311.9	315.1
	16		316.0	315.6
	18		64.0*	96.3
	20		185.4	197.9
	22		398.0	400.2
	24		58.2*	103.7
1	1	2	24.6*	22.1
	2		27.6*	8.0
	3		30.8*	13.4
	4		34.5*	27.3
	5		137.9	142.9
	6		42.3*	83.2
	7		141.9	146.0
	8		186.3	165.3
	9		53.5*	28.0
	10		57.1*	21.0
	11		60.8*	99.4
	12		159.2	126.4
	13		272.5	310.8
	14		306.9	284.0
	15		73.2*	80.4
	16		266.3	141.3
	17		77.0*	6.1
	18		77.8*	95.3
	19		76.9*	119.9
	20		134.0	164.7
	21		73.0*	9.0
	22		149.0	176.6
	23		66.7*	44.0
	24		140.8	162.9
2	0	2	135.7	152.7
	1		33.7*	41.2
	2		34.1*	26.5
	3		35.3*	74.5
	4		110.8*	158.8
	5		385.9	436.8
	6		108.5*	112.5
	7		235.0	265.1
	8		51.5*	51.0
2	9	2	143.1	108.0
	10		283.5	278.1
	11		724.1	709.8
	12		198.5	195.2
	13		147.4	139.7
	14		71.6*	74.6
	15		74.3*	37.9
	16		170.2	189.9
	17		440.6	484.4
	18		78.0*	118.6
	19		136.5	141.5
	20		75.0*	50.8
	21		72.2*	82.7
	22		156.0	189.1
	23		138.9	104.7
	24		55.5*	52.4
3	1	2	106.3*	144.9
	2		43.2*	11.9
	3		357.5	385.3
	4		51.4*	105.5
	5		238.0	260.2
	6		152.9	119.3
	7		53.9*	116.1
	8		54.7*	62.0
	9		225.8	254.4
	10		138.6	122.8
	11		64.3*	32.2
	12		67.5*	29.5
	13		70.4*	22.7
	14		73.1*	10.3
	15		75.0*	34.7
	16		148.9	110.3
	17		140.9	107.6
	18		78.4*	109.4
	19		77.0*	41.4
	20		74.5*	118.2
	21		181.5	81.8
	22		68.2*	46.0
	23		186.6	183.4
	24		130.8	152.6
4	0	2	554.9	590.9
	1		472.0	403.3
	2		215.7	202.3
	3		48.3*	17.6
	4		264.3	310.9
	5		426.3	468.6
	6		434.5	494.6
	7		279.5	316.4
	8		136.8	103.8
	9		213.9	185.9
	10		63.1*	81.2
	11		251.2	246.5
	12		68.6*	29.4
	13		71.5*	63.4
	14		182.3	268.5
	15		75.3*	5.5
	16		139.0	124.1
	17		77.2*	25.8
	18		220.8	238.2
	19		75.0*	7.8
	20		248.1	244.5
	21		178.4	195.7
	22		143.2	125.5
	23		59.2*	58.5
	24		45.4*	26.1
5	1	2	187.4	188.3
	2		270.5	274.9
	3		156.1	136.9
	4		54.6*	74.8
	5		155.0	105.4
	6		154.1	200.8
	7		177.3	193.6
	8		344.4	388.7
	9		327.2	359.5
	10		65.6*	53.4
	11		68.3*	28.2
	12		155.8	147.2
	13		151.2	138.6
	14		373.7	383.6
	15		251.1	269.2
	16		77.2*	71.4
	17		77.1*	41.6
	18		76.1*	43.0
	19		73.7*	67.2
	20		252.3	303.7
	21		188.5	233.2
	22		54.0*	120.1
	23		53.8*	28.9
6	0	2	132.4	131.2
	1		143.0	158.1
	2		243.2	168.8
	3		216.7	185.2
	4		61.7*	30.4
	5		186.6	191.6
	6		63.9*	10.0
	7		306.9	328.0
	8		67.1*	153.7
	9		320.0	335.4
	10		213.7	223.5
	11		201.6	237.8
6	12	2	77.1*	115.6
	13		76.3*	108.2
	14		77.4*	18.5
	15		298.9	284.3
	16		188.6	253.5
	17		124.6	135.3
	18		74.2*	140.8
	19		71.0*	49.8
	20		66.7*	81.8
	21		62.1*	45.0
	22		51.4*	91.5
	23		45.5*	27.4
7	1	2	123.5	113.0
	2		413.2	348.1
	3		273.5	269.6
	4		446.6	444.8
	5		68.8*	15.3
	6		70.1*	116.7
	7		71.2*	123.2
	8		158.4	153.0
	9		73.6*	95.4
	10		381.8	413.8
	11		76.2*	98.5
	12		150.9	131.7
	13		78.2*	81.9
	14		78.5*	73.4
	15		77.9*	101.1
	16		76.9*	15.1
	17		74.7*	14.4
	19		68.2*	85.6
	20		200.6	236.8
	21		113.9	161.0
	22		123.7	136.0
8	0	2	212.7	215.9
	1		252.2	236.8
	2		261.3	309.5
	3		217.7	209.7
	4		136.3	124.3
	5		72.7*	155.3
	6		74.0*	125.2
	7		75.4*	64.2
	8		227.0	117.4
	9		292.7	285.3
	10		79.3*	54.0
	11		80.1*	70.3
	12		80.6*	43.7
	13		80.7*	49.1
	14		80.1*	135.3
	15		78.9*	228.7
	16		299.7	74.5
	17		75.0*	109.0
	18		70.2*	63.2
	19		67.9*	42.0
	20		118.6	174.9
	21		52.1*	32.8
	22		36.7*	142.8
9	1	2	301.8	248.1
	2		282.6	210.8
	3		73.5*	149.0
	4		281.6	243.6
	5		76.1*	11.0
	6		77.2*	66.3
	7		278.5	319.3
	8		79.9*	35.7
	9		252.4	263.4
	10		250.2	242.9
	11		82.4*	84.8
	12		82.4*	157.1
	13		214.5	249.4
	14		80.4*	6.6
	15		321.1	416.5
	16		168.1	134.3
	17		72.1*	12.4
	18		67.3*	113.9
	19		121.6	141.0
	20		53.4*	64.7
10	0	2	74.5*	69.0
	1		174.7	195.9
	2		162.3	169.5
	3		176.6	130.1
	4		321.1	124.1
	5		276.5	310.5
	6		79.0*	38.9
	7		79.7*	79.0
	8		80.1*	55.8
	9		259.2	288.8
	10		80.8*	98.3
	11		252.2	324.9
	12		79.4*	17.8
	13		78.0*	82.9
	14		164.1	119.8
	15		72.9*	92.1
	16		200.7	187.3
	17		64.5*	76.1
	18		58.5*	92.7
	19		51.1*	22.5
11	1	2	351.5	359.4
	2		310.9	99.0
	3		76.9*	43.6
	4		255.0	337.2

Table 4. *(Continued)*

h	k	l	F_o	F_c	h	k	l	F_o	F_c	h	k	l	F_o	F_c	h	k	l	F_o	F_c	h	k	l	F_o	F_c
11	5	2	275.4	202.9	15	5	2	192.6	213.9	2	19	3	185.0	133.5	5	20	3	176.9	217.8	9	7	3	301.1	408.3
	6		78.8*	58.3		6		54.8*	75.6		20		57.1*	29.3	6	1	3	68.3*	19.3		8		75.8*	73.3
	7		223.3	233.7		7		53.2*	60.0		21		49.7*	16.6		2		362.7	320.2		9		75.0*	94.5
	8		78.8*	93.5		8		50.9*	99.7	3	0	3	133.4	141.4		3		67.6*	19.9		10		73.9*	118.7
	9		78.6*	113.2		9		48.0*	20.5		1		48.9*	34.6		4		209.1	212.5		11		72.3*	38.3
	10		178.3	188.1		10		44.2*	108.2		2		307.1	291.6		5		67.7*	93.8		12		158.9	134.9
	11		76.8*	62.9		11		38.8*	95.3		3		183.0	229.4		6		209.3	225.1		13		143.6	197.1
	12		75.0*	43.5	16	0	2	140.2	165.4		4		231.5	246.9		7		156.8	120.7		14		64.3*	26.1
	13		74.0*	102.8		1		46.0*	101.2		5		49.4*	79.8		8		161.9	143.5		15		60.3*	111.9
	14		69.5*	62.4		2		152.6	155.3		6		129.3	114.2		9		70.9*	37.5		16		148.5	190.6
	15		169.2	202.9		3		168.2	55.3		7		206.1	238.6		10		71.5*	82.3		17		45.6*	6.7
	16		61.2*	43.8		4		164.1	104.0		8		51.4*	139.3		11		136.7	145.6		18		24.5*	36.4
	17		156.1	138.2		5		213.7	256.0		9		327.4	397.7		12		229.3	227.7	10	1	3	77.3*	14.7
	18		47.9*	14.3		6		134.8	103.2		10		63.2*	62.3		13		72.1*	11.5		2		77.2*	99.4
12	0	2	203.4	164.2		7		37.5*	39.2		11		65.3*	77.4		14		71.6*	54.5		3		77.1*	9.1
	1		157.0	220.1		8		138.4	168.6		12		131.6	99.1		15		69.7*	65.4		4		76.8*	30.1
	2		109.4*	147.5	0	2	3	134.3	195.0		13		279.8	321.0		16		66.9*	21.4		5		76.4*	24.9
	3		136.7	56.1		4		38.7*	15.4		14		68.5*	33.9		17		148.8	149.1		6		313.1	306.6
	4		75.8*	26.9		6		238.4	239.7		15		256.8	249.5		18		58.6*	54.1		7		207.1	167.8
	5		167.3	168.3		8		519.3	469.8		16		251.7	196.2		19		56.6*	37.8		8		125.3	164.3
	6		76.2*	109.7		10		36.0*	25.9		17		249.6	246.5		20		40.5*	26.3		9		72.9*	10.4
	7		75.8*	94.3		12		138.6	200.1		18		262.7	246.4	7	0	3	74.6*	27.4		10		72.3*	16.7
	8		135.8	174.1		14		328.3	347.4		19		219.2	147.7		1		73.6*	61.2		11		70.4*	23.9
	9		74.3*	109.4		16		202.0	168.7		20		54.9*	30.1		2		380.8	377.7		12		193.1	299.3
	10		173.3	250.4		18		268.8	275.1		21		47.4*	52.8		3		72.9*	61.6		13		148.5	177.9
	11		156.3	141.7		20		168.2	183.7	4	1	3	55.3*	64.7		4		366.0	351.8		14		59.6*	22.8
	12		135.9	140.4		22		247.5	266.6		2		54.5*	32.7		5		72.8*	94.4		15		53.9*	117.1
	13		65.8*	16.7	1	0	3	22.7*	57.6		3		218.2	222.7		6		171.7	164.8		16		44.5*	49.6
	14		62.4*	87.0		1		24.6*	63.2		4		54.7*	108.7		7		73.7*	62.8	11	0	3	144.0	158.1
	15		57.7*	28.6		2		204.1	296.5		5		127.6	161.9		8		73.9*	32.5		1		145.1	161.0
	16		220.8	264.6		3		30.9*	123.8		6		57.2*	43.2		9		187.9	199.1		2		70.0*	54.8
	17		43.4*	15.9		4		179.9	195.0		7		149.5	186.4		10		273.8	312.2		3		70.8*	42.8
13	1	2	70.7*	28.0		5		300.1	291.7		8		61.5*	85.8		11		75.6*	64.4		4		199.2	233.2
	2		71.4*	11.2		6		47.4*	16.8		9		63.4*	79.9		12		328.3	404.4		5		232.3	234.3
	3		188.6	193.5		7		234.5	215.9		10		65.4*	18.6		13		72.3*	111.8		6		73.1*	56.8
	4		150.6	188.5		8		278.8	244.6		11		67.2*	117.3		14		126.3	124.0		7		152.8	156.3
	5		72.1*	9.9		9		267.8	215.1		12		68.9*	90.5		15		133.5	194.5		8		71.9*	6.6
	6		125.6	166.9		10		61.3*	86.0		13		369.7	342.3		16		126.3	150.0		9		106.5	74.6
	7		71.0*	61.0		11		122.3	107.6		14		69.7*	94.8		17		113.5	77.4		10		133.6	126.7
	8		71.9*	53.2		12		65.8*	9.9		15		164.1	157.0		18		350.5	408.2		11		120.3	191.3
	9		68.3*	29.9		13		266.7	257.2		16		170.7	157.4		19		44.2*	118.6		12		195.2	211.1
	10		232.1	262.4		14		68.7*	23.8		17		66.7*	69.8	8	1	3	261.7	231.3		13		116.2	52.4
	11		63.7*	90.3		15		141.4	85.8		18		64.4*	5.5		2		75.6*	62.9		14		43.4*	42.4
	12		169.2	198.5		16		193.9	213.6		19		59.6*	253.0		3		75.7*	40.5	12	1	3	177.8	90.8
	13		56.7*	7.7		17		68.2*	33.7		20		53.7*	48.6		4		75.5*	108.7		2		210.2	209.2
	14		51.9*	81.7		18		66.3*	13.6		21		42.9*	67.2		5		221.2	272.1		3		230.5	234.6
	15		177.3	200.6		19		127.3	172.5	5	0	3	213.2	214.0		6		75.6*	35.2		4		238.4	255.7
14	0	2	375.8	374.8		20		61.8*	149.9		1		303.1	274.9		7		75.6*	24.4		5		142.0	138.9
	1		180.4	226.9		21		139.6	127.5		2		383.9	360.9		8		75.3*	38.4		6		62.7*	9.6
	2		65.7*	16.4	2	1	3	181.8	201.6		3		61.6*	57.2		9		75.1*	33.6		7		61.4*	99.9
	3		65.9*	93.8		2		163.8	197.4		4		250.5	241.3		10		74.6*	58.4		8		129.6	114.1
	4		65.9*	74.3		3		335.5	437.2		5		60.9*	29.5		11		73.5*	23.2		9		129.3	103.4
	5		273.5	164.0		4		254.6	293.9		6		118.3	151.6		12		74.0*	9.2		10		141.5	198.0
	6		193.5	256.3		5		288.9	324.1		7		309.1	333.3		13		151.8	166.3		11		53.0*	35.9
	7		64.1*	60.1		7		161.6	121.1		8		155.9	140.9		14		67.9*	28.8		12		48.3*	8.3
	8		62.2*	99.3		8		223.4	232.5		9		177.9	199.1		15		63.5*	52.7	13	0	3	164.0	206.9
	9		141.6	145.0		9		251.6	265.0		10		67.7*	39.8		16		58.9*	117.1		1		54.2*	96.4
	10		190.7	217.8		10		163.8	110.7		11		67.9*	85.6		17		197.6	187.4		2		54.2*	52.3
	11		126.6	9.9		11		283.9	279.0		12		69.1*	36.1		18		46.4*	38.9		3		54.2*	29.9
	12		126.7	170.0		12		65.6*	19.6		13		288.0	264.5	9	0	3	78.7*	105.8		4		53.4*	7.8
	13		44.2*	29.6		13		67.2*	74.3		14		68.6*	25.8		1		329.4	334.7		5		131.5	100.4
	14		126.6	108.0		14		168.8	168.9		15		164.0	141.6		2		305.1	80.1		6		191.0	118.2
15	1	2	182.3	201.4		15		68.3*	75.8		16		68.2*	30.3		3		77.4*	52.7		7		166.7	202.3
	2		56.7*	21.4		16		67.9*	5.3		17		66.2*	79.4		4		77.2*	4.2		8		48.1*	67.4
	3		56.7*	72.8		17		66.7*	43.0		18		62.7*	6.6		5		150.8	131.1		9		45.2*	35.8
	4		173.2	92.6		18		252.7	96.6		19		58.2*	72.9		6		289.0	196.4		10		40.8*	2.0

Results of the refinement

The asymmetric unit of the structure of nuffieldite contains 13 atoms: five heavy-metal atoms [designated M(1) through M(5)], one Cu atom, and seven sulfur atoms, all located in special position 4 *c m* of space group *Pbnm*. The temperature factors for the metal atoms are between 1 and 2 Å^2. Such values are typical for the bismuth sulfosalts whose structures are known. Scattering from the mineral is dominated by these metal atoms, since they account for eighty percent of the electron density contained within the cell. Accordingly the temperature factors obtained for the sulfur atoms display very high standard deviations, and the individual values which were obtained have little significance. We can, for similar reasons, provide no evidence for a partially-occupied site which might cause the cell content to be closer to 27 sulfur atoms rather than the 28 required by the space group.

Table 5. *Interatomic distances in nuffieldite*

(Standard deviations in parentheses; distance to second-nearest neighbors in brackets)

a) Metal-atom polyhedra

M(1) = (Pb + Bi)			M(2) = (Pb)			M(3) = (Pb)		
S(2)	2.67(5) Å		S(4)′	2.74(3) Å	2×	S(3)	2.77(4) Å	
S(6)′	2.90(4)	2×	S(1)	2.92(7)		S(3)‴	3.00(3)	2×
S(1)′	3.00(5)	2×	S(2)′	2.92(3)	2×	S(5)′	3.02(3)	2×
[S(4)′	3.33(3)	2×]	S(7)	3.01(4)		[S(6)‴	3.33(6)]	
			[S(5)	3.68(4)]		[S(7)′	3.37(3)	2×]

M(4) = (Bi)			M(5) = (Bi)			Cu		
S(7)‴	2.60(3) Å	2×	S(5)‴	2.74(4) Å		S(4)	2.25(4) Å	
S(6)	2.62(6)		S(3)′	2.76(2)	2×	S(5)′	2.26(2)	2×
S(2)′	2.99(3)	2×	S(1)‴	2.93(5)	2×	S(1)	2.32(7)	
]S(2)‴	3.43(5)]		[S(6)	3.25(6)]		[S(3)	3.82(4)]	
			[S(4)	3.30(4)]				

b) Sulfur-atom polyhedra

S(1)			S(2)			S(3)		
Cu	2.32(7) Å		M(1)	2.67(5) Å		M(5)′	2.76(2) Å	2×
M(2)	2.92(7)		M(2)‴	2.92(3)	2×	M(3)	2.77(4)	
M(5)′	2.93(5)	2×	M(4)′	2.99(4)	2×	M(3)‴	3.00(3)	2×
M(1)′	3.00(5)	2×	[M(4)$^{\mathrm{VI}}$	3.43(5)]		[Cu	3.82(4)]	

S(4)			S(5)			S(6)		
Cu	2.25(4) Å		Cu′	2.26(2) Å	2×	M(4)	2.62(6) Å	
M(2)′	2.74(3)	2×	M(5)‴	2.74(4)		M(1)′	2.90(4)	2×
[M(5)	3.30(4)]		M(3)′	3.02(3)	2×	[M(5)	3.25(6)]	
[M(1)′	3.33(3)	2×]	[M(2)	3.68(4)]		[M(3)‴	3.33(6)]	

S(7)		
M(4)$^{\mathrm{VI}}$	2.60(3) Å	2×
M(2)	3.01(4)	
[M(3)′	3.37(3)	2×]
[M(4)	4.15(4)]	

The bond distances and angles in the structure are presented in Tables 5 and 6, respectively. The geometry of the coordination polyhedra is depicted in Fig. 1. The Cu atom is tetrahedrally coordinated,

Table 6. *Bond angles in nuffieldite*
(Estimated standard deviations in parentheses)

M(1) = (Pb,Bi)			M(2) = Pb		
S(4)′—M(1)—S(6)″	67.7(12)°	2×	S(1) —M(2)—S(2)″	79.6(13)°	2×
S(1)′—M(1)—S(4)′	72.8(13)	2×	S(2)′ —M(2)—S(7)	81.7(10)	2×
S(4)′—M(1)—S(4)″	74.8 (8)		S(2)′ —M(2)—S(2)″	87.8(13)	
S(1)′—M(1)—S(2)	82.2(14)	2×	S(4)′ —M(2)—S(2)′	87.9 (9)	2×
S(1)′—M(1)—S(1)″	84.9(18)		S(4)′ —M(2)—S(1)	91.3(12)	2×
S(2) —M(1)—S(6)′	86.4(15)	2×	S(4)′ —M(2)—S(4)″	95.1(12)	
S(6)′—M(1)—S(6)″	88.6(17)		S(4)″—M(2)—S(7)	106.1 (9)	2×
S(1)′—M(1)—S(6)″	92.1(12)	2×			
S(4)′—M(1)—S(6)″	118.0(13)	2×			
S(1)′—M(1)—S(4)″	121.6(13)	2×			

M(3) = Pb			M(4) = Bi		
S(5)′ —M(3)—S(7)′	60.5(11)°	2×	S(2)‴—M(4)—S(7)‴	78.8(10)°	2×
S(6)‴—M(3)—S(3)‴	72.5(10)	2×	S(2)′ —M(4)—S(2)″	85.3(12)	
S(7)′ —M(3)—S(7)″	73.7 (8)		S(2)′ —M(4)—S(6)	85.6(13)	2×
S(3) —M(3)—S(5)′	78.0 (9)	2×	S(2)′ —M(4)—S(7)^{IV}	86.1 (9)	2×
S(3) —M(3)—S(3)‴	81.0 (9)	2×	S(6) —M(4)—S(7)‴	91.2(12)*	2×
S(5)′ —M(3)—S(5)″	84.1(11)		S(7)^{IV}—M(4)—S(7)‴	102.4(14)*	
S(3)‴—M(3)—S(3)^{IV}	84.7 (9)		S(2)′ —M(4)—S(2)‴	106.1(9)	2×
S(5)′ —M(3)—S(3)‴	91.8 (8)	2×			
S(7)′ —M(3)—S(5)″	108.0(11)	2×			
S(6)‴—M(3)—S(5)′	126.1 (9)	2×			

M(5) = Bi			Cu		
S(6) —M(5)—S(3)′	64.4(12)°		S(1) —Cu—S(5)′	97.3(15)°	2×
S(1)‴—M(5)—S(5)‴	74.5(15)		S(5)′ —Cu—S(4)	110.7(13)	2×
S(6) —M(5)—S(3)′	76.8 (9)	2×	S(1) —Cu—S(4)	110.9(22)	
S(1)^{IV}—M(5)—S(4)	80.9(14)	2×	S(5)″—Cu—S(5)′	127.2(22)	
S(3)′ —M(5)—S(5)‴	83.0 (9)*	2×			
S(1)^{IV}—M(5)—S(3)″	84.9(11)	2×			
S(1)‴—M(5)—S(1)^{IV}	87.3(18)				
S(3)′ —M(5)—S(3)″	94.2(11)*				
S(3)″ —M(5)—S(4)	118.6(8)	2×			
S(6) —M(5)—S(1)‴	124.6(13)	2×			
S(4) —M(5)—S(5)‴	145.6(11)				

Table 6. *(Continued)*

S(1)			S(2)		
M(1)′—S(1)—Cu	80.8(18)°	2×	M(4)′ —S(2)—M(4)$^{\text{V}}$	73.9 (9)°	2×
M(1)′—S(1)—M(1)″	84.9(18)		M(4)′ —S(2)—M(4)″	85.3(12)	
M(5)′—S(1)—M(5)″	87.3(18)		M(2)‴—S(2)—M(2)$^{\text{IV}}$	87.8(13)	
M(5)′—S(1)—Cu	87.7(18)	2×	M(2)‴—S(2)—M(4)$^{\text{V}}$	90.7(11)	2×
M(1)′—S(1)—M(5)′	92.7 (3)	2×	M(2)$^{\text{IV}}$—S(2)—M(4)″	91.4 (3)	2×
M(2) —S(1)—M(1)″	95.4(16)	2×	M(1) —S(2)—M(4)′	92.4(12)	2×
M(2) —S(1)—M(5)′	96.1(17)	2×	M(1) —S(2)—M(2)‴	102.8(12)	2×

S(3)			S(4)		
M(3)$^{\text{IV}}$—S(3)—M(3)‴	84.7 (9)°		M(1)″—S(4)—Cu	74.5(10)°	2×
M(5)‴—S(3)—M(3)$^{\text{IV}}$	86.6 (3)	2×	M(1)″—S(4)—M(1)′	74.8(8)	
M(5)′ —S(3)—M(5)″	94.2(11)		M(5) —S(4)—M(2)″	91.6 (9)	2×
M(3) —S(3)—M(3)$^{\text{IV}}$	99.0 (9)	2×	M(1)″—S(4)—M(5)	92.8 (8)	2×
M(5)″ —S(3)—M(3)	102.1 (9)	2×	M(1)″—S(4)—M(2)″	94.9 (3)	2×
			M(2)″—S(4)—M(2)′	95.1(12)	
			Cu —S(4)—M(2)″	99.2(11)	2×

S(5)			S(6)		
Cu″ —S(5)—M(3)″	73.5 (7)°		M(3)‴—S(6)—M(5)	73.9(13)°	
Cu′ —S(5)—M(3)′	73.5 (7)		M(4) —S(6)—M(3)‴	80.6(15)	
M(3)″ —S(5)—M(3)′	84.1(11)		M(1)″ —S(6)—M(1)′	88.6(17)	
M(5)‴—S(5)—Cu	93.7(14)	2×	M(1)″ —S(6)—M(4)	95.6(16)	2×
M(5)‴—S(5)—M(3)″	96.4(11)	2×	M(1)″ —S(6)—M(5)	102.5(15)	2×
Cu″ —S(5)—Cu′	127.2(22)		M(1)″ —S(6)—M(3)‴	135.7 (8)	2×

S(7)		
M(3)″ —S(7)—M(3)′	73.7(8)°	
M(4)$^{\text{IV}}$—S(7)—M(3)″	80.1(5)	2×
M(4)$^{\text{IV}}$—S(7)—M(4)‴	102.4(14)	
M(2) —S(7)—M(4)$^{\text{IV}}$	107.5(10)	2×
M(2) —S(7)—M(3)″	110.1(10)	2×
M(4)$^{\text{IV}}$—S(7)—M(3)″	139.6(14)	2×

* angles between three shortest bonds.

with sulfur atoms at fairly uniform distances of 2.25—2.32 Å. Three of the six bond angles are nearly the same as the ideal tetrahedral angle of 109.47°. All of the heavy-metal atoms are coordinated by five sulfur atoms within a distance of 3.02 Å with the exception of M(2) which has six neighbors within this range. Lead and bismuth have virtually identical scattering power ($Z = 82$ and 83, respectively) but may be distinguished through slight differences in the geometry of their coordination polyhedra. The distance of closest approach of a sulfur atom to Pb seldom falls below 2.8 Å, while minimum Bi—S distances are observed to be in the range 2.5—2.6 Å. Moreover, the Bi coordination polyhedron usually displays three bonds of this magnitude with the orthogonal disposition which is characteristic of Group V metals. Since 2 and 1/2 atoms of each specie are to be assigned to the five sites of nuffieldite, it is clear that some, but not all, of the Pb and Bi atoms may be ordered. Inspection of Tables 5 and 6 shows that M(4) displays three short orthogonal bonds of 2.60 and 2.62 (2 ×) Å. This site must contain Bi. Similarly M(5) displays three short, nearly equal bonds of 2.74 and 2.76 (2 ×) Å which, though large compared to those of M(4), correspond to values which have been observed in a few Bi sulfosalts [*e.g.*, 2.78 and 2.79 Å for Bi(2) in galenobismutite (IITAKA and NOWACKI, 1966)]. For M(2) and M(3) no trio of short bonds is present. With the exception of a single relatively short distance of 2.74 Å for M(2) and 2.77 Å for M(3), all bond lengths are between 2.92 and 3.02 Å. Therefore M(2) and M(3) are designated as Pb. The fifth heavy atom, M(1), has a peculiar coordination scheme. It displays a single short bond of 2.67 Å which is too short for Pb and quite typical of a Bi—S separation. However, the next-largest bond lengths, 2.90 Å, are quite large compared with the intermediate bonds in other Bi polyhedra. A statistical occupancy of Pb and Bi is therefore assigned to this site. Disordered arrangments of Pb and Bi are not uncommon. For example, attempts to synthesize the ordered intermediate phases in the system Bi_2S_3—$PbCuBiS_3$ (bismuthinite—aikinite) produced only disordered solid solutions (SPRINGER,

Table 7
Comparison of bond distances for sites believed to contain disordered Pb *and* Bi

Mineral	Atom	Bond lengths (Å)	Reference
nuffieldite	M(1)	2.67, 2.90(2×), 3.00(2×) 3.33(2×)	present work
lillianite, $Pb_3Bi_2S_6$	M(1)	2.69, 2.80(2×), 2.98(2×) 2.99	TAKAGI and
	M(2)	2.64, 2.82(2×), 2.94(2×) 3.27	TAKÉUCHI (1972)
$PbCu_4Bi_5S_{11}$	M(1)	2.79(2×), 2.84(4×)	KUPČIK and
	M(2)	2.80(4×), 2.82(2×)	MACKOVICKÝ (1968)

1971). Two additional structure determinations—$PbCu_4Bi_5S_{11}$ (Kupčik and Makovický, 1968) and lillianite, $Pb_3Bi_2S_6$ (Takagi and Takéuchi, 1972)—have also produced results which must be interpreted as indicating Pb, Bi disorder. The coordination of these sites, Table 7, presents peculiarities similar to those observed for M(1).

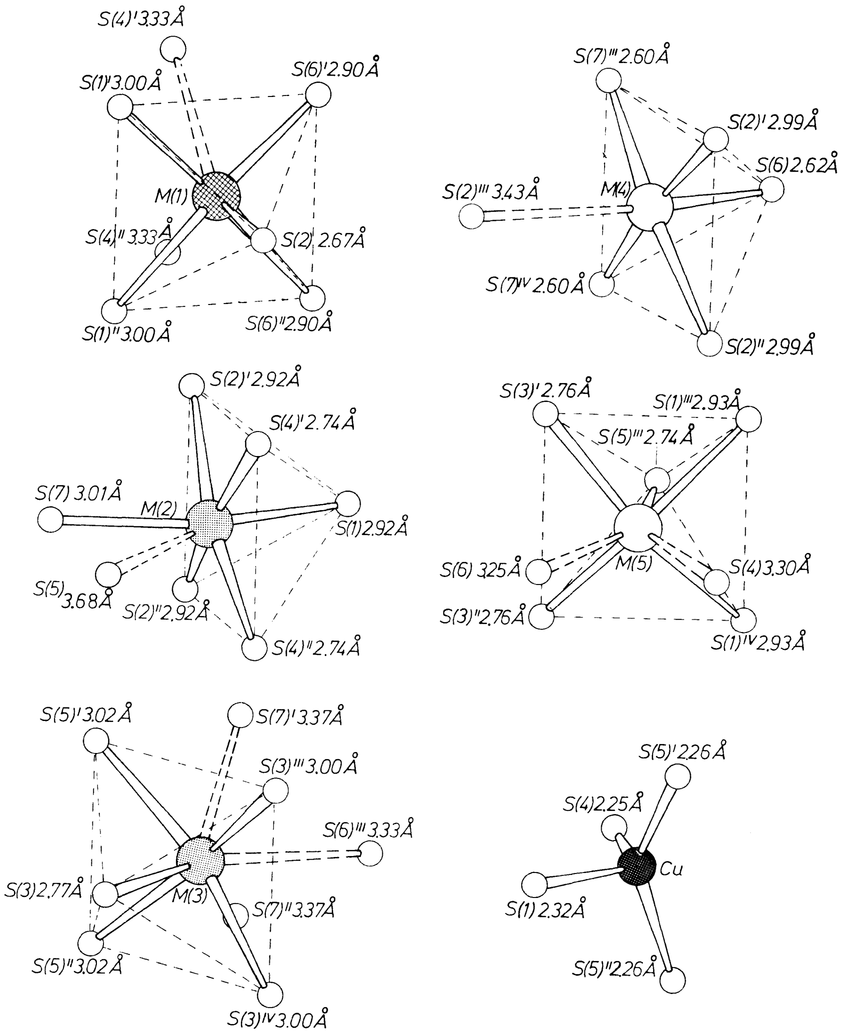

Fig. 1*a*

Fig. 1. Coordination polyhedra in nuffieldite. (*a*) Arrangement of sulfur atoms about the metal atoms. (*b*) Arrangement of metal atoms about the sulfur atoms

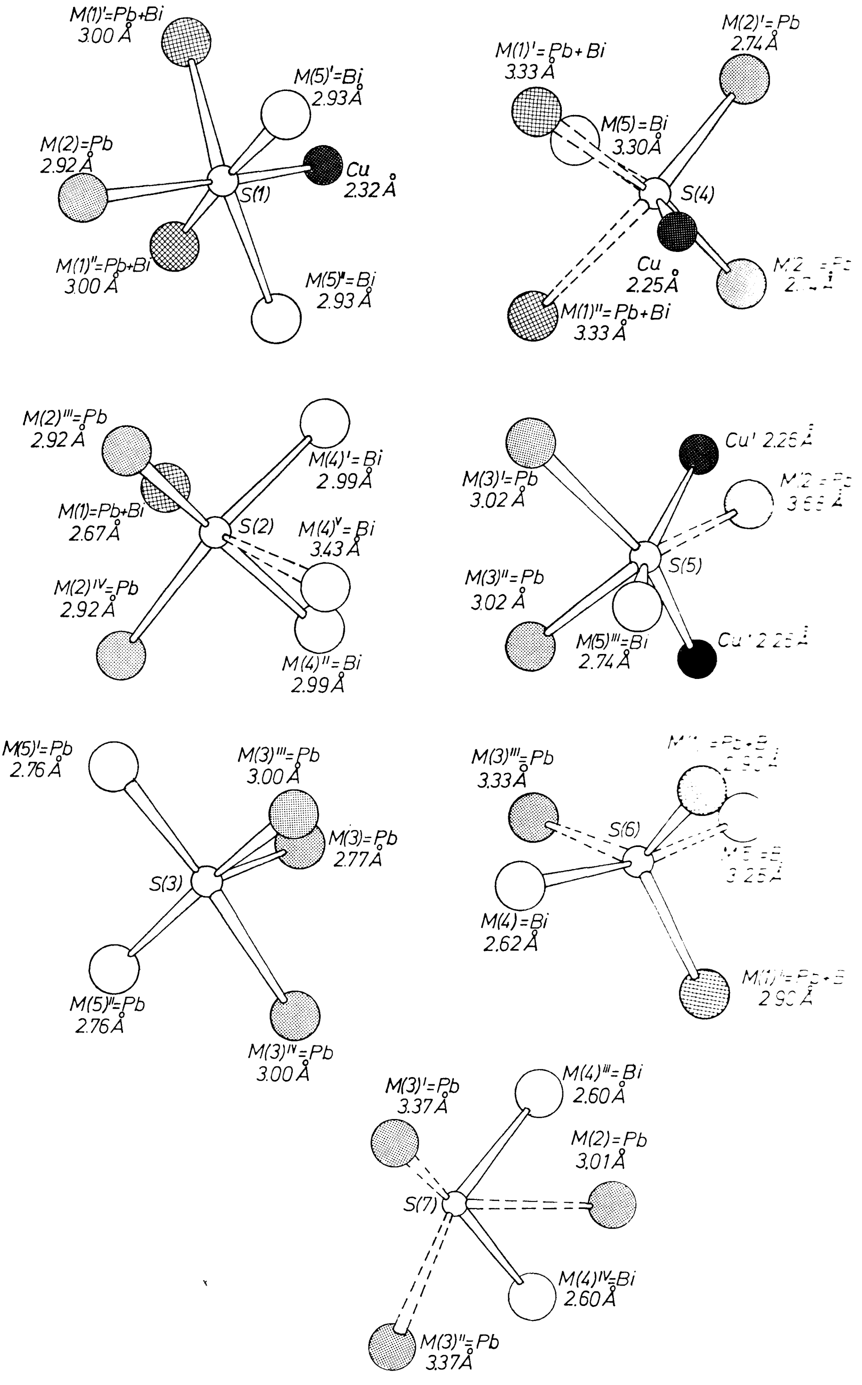
M(1)'=Pb+Bi 3.00 Å
M(5)'=Bi 2.93 Å
M(2)=Pb 2.92 Å
Cu 2.32 Å
S(1)
M(1)''=Pb+Bi 3.00 Å
M(5)''=Bi 2.93 Å
M(1)'=Pb+Bi 3.33 Å
M(2)'=Pb 2.74 Å
M(5)=Bi 3.30 Å
S(4)
Cu 2.25 Å
M(1)''=Pb+Bi 3.33 Å
M(2)'''=Pb 2.92 Å
M(4)'=Bi 2.99 Å
M(1)=Pb+Bi 2.67 Å
S(2)
M(4)^V=Bi 3.43 Å
M(2)^IV=Pb 2.92 Å
M(4)''=Bi 2.99 Å
Cu' 2.26 Å
M(3)'=Pb 3.02 Å
S(5)
M(3)''=Pb 3.02 Å
M(5)'''=Bi 2.74 Å
Cu' 2.26 Å
M(5)'=Pb 2.76 Å
M(3)'''=Pb 3.00 Å
M(3)=Pb 2.77 Å
S(3)
M(5)''=Pb 2.76 Å
M(3)^IV=Pb 3.00 Å
M(3)'''=Pb 3.33 Å
S(6)
M(5)=Bi 3.25 Å
M(4)=Bi 2.62 Å
M(1)''=Pb+Bi 2.90 Å
M(3)'=Pb 3.37 Å
M(4)'''=Bi 2.60 Å
M(2)=Pb 3.01 Å
S(7)
M(4)^IV=Bi 2.60 Å
M(3)''=Pb 3.37 Å

Fig. 1b

Table 8. *Sulfur-sulfur separation in metal-atom coordination polyhedra*
(The presence of a metal atom following the separation indicates that the edge is shared with that coordination polyhedron; estimated standard deviations in parentheses)

M(1) = Pb + Bi				M(2) = Pb			
S(4)′–S(6)′	3.49(7) Å	2×	M(5)	S(5) –S(7)	3.23(6) Å		M(3)
S(2) –S(1)′	3.73(7)	2×	M(2)	S(5) –S(4)′	3.71(5)	2×	Cu
S(4)′–S(1)′	3.76(8)	2×	Cu	S(1) –S(2)′	3.73(6)	2×	M(1)
S(2) –S(6)′	3.82(7)	2×	M(4)	S(7) –S(2)′	3.88(5)	2×	
S(1)′–S(1)″	4.00(0)	= c	M(5)	S(2)′–S(4)′	3.93(6)	2×	M(2)
S(6)′–S(6)″	4.00(0)	= c		S(2)′–S(2)″	4.00(0)	= c	M(4)
S(4)′–S(4)″	4.00(0)	= c		S(4)′–S(4)″	4.00(0)	= c	M(1)
S(1)′–S(6)′	4.24(9)	2×	M(1)	S(1) –S(4)′	4.05(7)	2×	M(5)

M(3) = Pb				M(4) = Bi			
S(5)′ –S(7)′	3.23(6) Å	2×	M(2)	S(6) –S(7)‴	3.72(6) Å	2×	M(3)
S(3) –S(5)′	3.65(5)	2×	M(5)	S(6) –S(2)′	3.82(7)	2×	M(1)
S(6)‴–S(7)′	3.72(6)	2×	M(4)	S(7)‴–S(2)′	3.82(6)	2×	M(4)
S(3) –S(3)‴	3.75(6)	2×	M(3)	S(2)‴–S(7)‴	3.88(5)	2×	M(2)
S(6)‴–S(3)‴	3.75(6)	2×	M(5)	S(7)‴–S(7)$^{\mathrm{IV}}$	4.00(0)	= c	M(3)
S(5)′ –S(5)″	4.00(0)	= c	Cu	S(2)′ –S(2)″	4.00(0)	= c	M(2)
S(7)′ –S(7)″	4.00(0)	= c	M(4)				
S(3)‴–S(3)$^{\mathrm{IV}}$	4.00(0)	= c	M(5)				
S(7)′ –S(3)‴	4.42(5)	2×	M(3)				

M(5) = Bi				Cu			
S(5)‴–S(1)‴	3.44(6) Å	2×	Cu	S(1) –S(5)′	3.44(6) Å	2×	M(5)
S(6) –S(4)	3.49(7)		M(1)	S(5) –S(4)	3.71(5)	2×	M(2)
S(5)‴–S(3)′	3.65(5)	2×	M(3)	S(1) –S(4)	3.76(8)		M(1)
S(6) –S(3)′	3.75(6)	2×	M(3)	S(5)′–S(5)″	4.00(0)	= c	M(3)
S(3)′ –S(1)‴	3.84(7)	2×	M(5)				
S(3)′ –S(3)″	4.00(0)	= c	M(3)				
S(1)‴–S(1)$^{\mathrm{IV}}$	4.00(0)	= c	M(1)				
S(4) –S(1)‴	4.05(7)	2×	M(2)				

Table 8 presents the sulfur-sulfur atom separations in the metal-atom coordination polyhedra, along with an indication of whether this edge is shared with that of another polyhedron. Few distances are less than 3.70 Å, the van der Waals contact distance given by PAULING (1960), and none are smaller than the minimum intermolecular sulfur-sulfur contacts which have been previously observed (*e.g.* 3.20 Å in S_6, DONOHUE *et al.*, 1961). In contrast to ionic structures, there is little correlation between the length of a polyhedral edge and the fact that it is shared. This is usually the case in sulfosalt structures.

Discussion of the structure

A projection of the structure of nuffieldite along *c* is given in Fig. 2. The most significant feature of the structure is that it contains a four-membered chain of pyramids (indicated by hatching in Fig. 2.) of

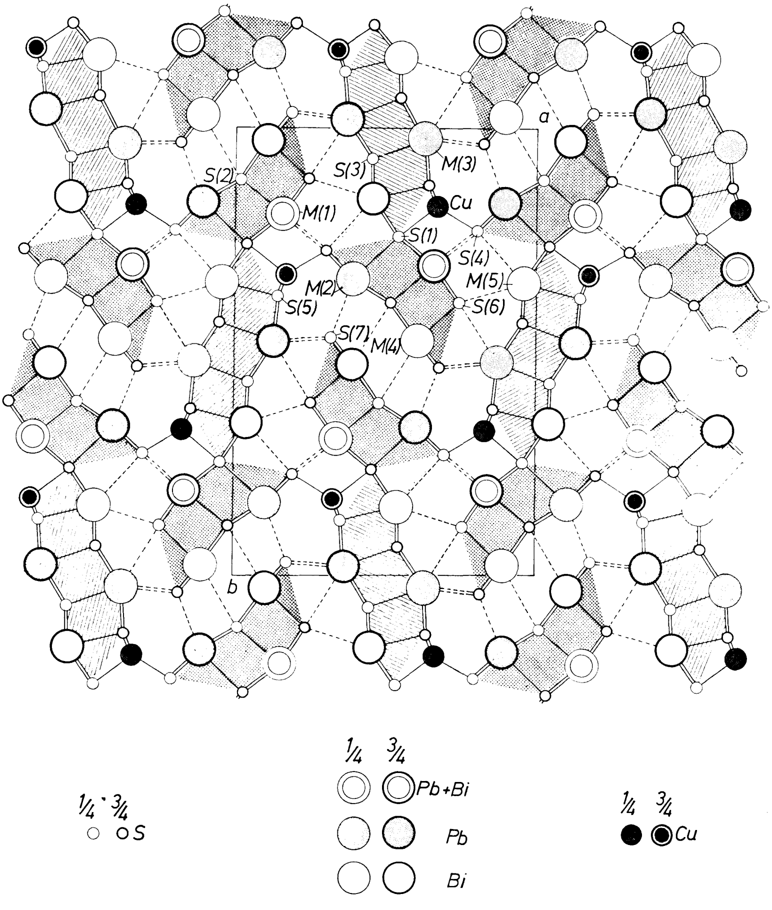

Fig. 2. The structure of nuffieldite projected along *c*. Hatched areas indicate four-membered chains identical to those found in aikinite; shaded areas indicate a three-membered chain. (A single line indicates a bond to an atom with the same *z* coordinate. Double lines indicate bonds to two atoms, superposed in projection, at $\Delta z = \pm \frac{1}{2}$. Dotted lines indicate weak interchain bonds of length greater than 3.3 Å)

composition $PbBiS_3$. This chain is a derivative of that found in the stibnite-type structure of bismuthinite, Bi_2S_3 (Kupčik and Veselá-Novaková, 1970), and along with its flanking chains of Cu tetrahedra, is *identical* to the structural unit found in aikinite, $PbCuBiS_3$ (Kohatsu and Wuensch, 1971). The nuffieldite structure, in addition, contains a second type of chain-like unit which is reminiscent of the stibnite structure. The chain (indicated in Fig. 2 by shading) is a new type of unit for sulfosalt structures and consists of a three-membered chain involving Pb, Bi and the disordered (Pb, Bi) site. Two of these three-membered chains share an edge with the aikinite-like chain to form a complex ten-membered chain. The arrangement of these chains within the cell is the same as that in bismuthinite and aikinite (which, indeed, have the same space group as nuffieldite). The ten-membered chains are linked by the Cu tetrahedra. Additional linkages are formed by weak bonds of separations greater than those of the five close nearest-neighbors about each heavy-metal atom (such is also the case in the stibnite structure type). The aikinite-like chain forms such weak bonds to only three-membered chains (plus one weak bond, M(5)—S(4), within the ten-membered chain). Each three-membered chain forms weak bonds to two other three-membered chains as well as to an aikinite-like chain.

All bismuth sulfides, as has been mentioned earlier, display a common 4 Å translation. This corresponds to the periodicity of a chain of BiS_5 square pyramids linked by the sharing of basal edges. Such compounds might therefore be expected to display some unifying structural theme. Too few structures are yet known to establish any complete crystal-chemical principle, yet certain trends are becoming apparent. The lead-bismuth sulfosalts with relatively high Pb content (Otto and Strunz, 1968; lillianite, $Pb_3Bi_2S_6$, Takagi and Takéuchi, 1972; cosalite, $Pb_2Bi_2S_5$, Weitz and Hellner, 1960) tend to contain thick (*i.e.*, one subcell or greater) slabs with structure closely related to that of PbS. Structures with high bismuth content, on the other hand, appear to form chain structures which are either derivatives of, or closely related to, the stibnite and bismuthinite structure types (*i.e.*, the rocksalt-like units are finite in extent and only one-half subcell in thickness). When the copper content is high, the structure consists of heavy metal chains linked by Cu-S regions which form an important feature of the structure (*e.g.*, emplectite, $CuBiS_2$, Kupčik 1965; Jenkins, 1969; $PbCu_4Bi_5S_{11}$, Kupčik and Makovický, 1968; $Cu_4Bi_4S_9$. Ozawa and Takéuchi, 1972). The Cu-S slabs may display

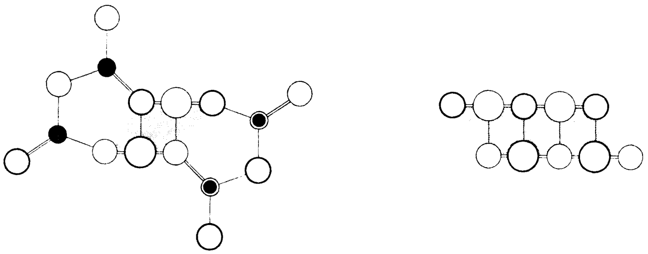

(a) emplectite, $CuBiS_2$

(b) bismuthinite, Bi_2S_3

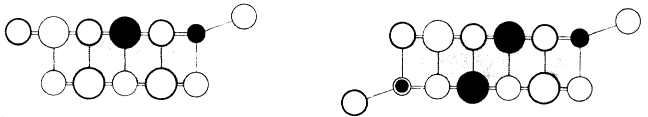

(c) gladite, $PbCuBi_5S_9$

(d) aikinite, $PbCuBiS_3$

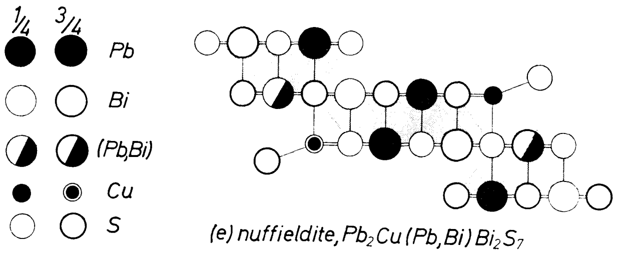

(e) nuffieldite, $Pb_2Cu(Pb,Bi)Bi_2S_7$

Fig. 3. Idealized representations of chains found in Bi-rich sulfosalts. (*a*) double chain found in emplectite, $CuBiS_2$, (*b*) quadruple chain found in bismuthinite, Bi_2S_3, (*c*) the Pb-containing chain in gladite, $PbCuBi_5S_9$, (*d*) the chain in aikinite, $PbCuBiS_3$, (*e*) the ten-membered chain found in nuffieldite

copper atoms in either three- or fourfold coordination and these regions display a structural resemblance to covellite, CuS (OZAWA and TAKÉUCHI, 1972). If the Cu content of the mineral is low, however, the Cu atoms appear to play a relatively passive role in the structure: They occupy tetrahedral sites between stibnite-like ribbons to form a single tetrahedral chain which shares an edge to extend the width of each ribbon.

Figure 3 summarizes in schematic and idealized form the ribbon-like units which have to date been found in the bismuth sulfides of high Bi content. A two-membered chain (Fig. 3*a*) which corresponds to the kernel of the stibnite chain occurs in emplectite, $CuBiS_2$, and in $Cu_4Bi_4S_9$. The four-membered chain in the stibnite-type structure of bismuthinite is shown in Fig. 3*b*. Aikinite displays a four-membered chain which is a derivative of the stibnite chain (Kohatsu and Wuensch, 1971) in which Pb replaces the Bi in the interior five-coordinated site in the chain. The Cu atom is added to a tetrahedral site such that it forms a tetrahedral chain adjacent to the Pb site, Fig. 3*d*. Gladite, $PbCuBi_5S_9$ (Kohatsu and Wuensch, 1973) consists of a mixture of bismuthinite chains and four-membered chains in which only one of the heavy-atom sites is occupied by Pb (Fig. 3*c*). It is of interest to note that the single flanking chain of Cu tetrahedra again occupies a position adjacent to the Pb site as in aikinite. A four-membered chain is also found in galenobismutite (Iitaka und Nowacki, 1962) but, in contrast, the Pb atoms were assigned to the exterior, three-coordinated, sites in the chain. Finally, Fig. 3*e* presents, in idealized form, the ten-membered chain discovered in nuffieldite. Its central portion is identical to the four-membered chain of aikinite with, again, the same flanking chain of Cu tetrahedra. It seems likely that the several additional complex bismuth sulfosalts with high Bi and low Cu content which have been recently reported—*e.g*, neyite, $Pb_7Cu_2Bi_6S_{17}$ (Drummond *et al.*, 1969); or berryite, $Pb_6Cu_9Bi_{15}S_{33}$ (Nuffield and Harris, 1966) may provide yet additional variations of extended ribbons similar to those found in nuffieldite.

Acknowledgments

The writers are pleased to thank Dr. P. W. Kingston for his generosity in supplying for study the remaining crystals of nuffieldite, and Dr. J. D. Scott for his continued interest in the problem. The contribution of one of us (I.K.) was supported, in part, by an I.B.M. Fellowship. This study was supported under Grant GA-22698A1 from the Earth Sciences Section of the U. S. National Science Foundation.

References

Charles W. Burnham (1962), Lattice constant refinement. Carnegie Inst. Washington Year Book **61**, 133—135.

Charles W. Burnham (1966), Computation of absorption corrections, and the significance of end effect. Amer. Mineral. **51**, 159—167.

J. Donohue, A. Caron and E. Goldish (1961), The crystal and molecular structure of S_6 (sulfur-6). J. Amer. Chem. Soc. **83**, 3748—3751.

A. D. Drummond, J. Trotter, R. M. Thompson and J. A. Gower (1969), Neyite, a new sulfosalt from Alice Arm, British Columbia. Canad. Mineral. **10**, 90—96.

E. B. Fleischer, R. B. K. Dewar and A. L. Stone (1967), Use of the symbolic addition method in the solution of centrosymmetric structures; description of a computer program to automate the process. Abstract A 7, Program and Abstracts, Winter Meeting of the Amer. Crystallogr. Assoc., 20.

Y. Iitaka and W. Nowacki (1962), A refinement of the crystal structure of galenobismutite, $PbBiS_4$. Acta Crystallogr. **15**, 691—698.

Judith K. Jenkins (1969), The crystal structure of emplectite, $CuBiS_2$, S. B. Thesis, Dept. of Metallurgy and Materials Science, Massachusetts Institute of Technology.

P. W. Kingston (1968), Studies of mineral sulphosalts: XXI. Nuffieldite, a new species. Canad. Mineral. **9**, 439—452.

Iwao Kohatsu and B. J. Wuensch (1971), the crystal structure of aikinite, $PbCuBiS_3$. Acta Crystallogr. B **27**, 1245—1252.

Iwao Kohatsu and B. J. Wuensch (1973), The crystal structure of gladite, $PbCuBi_5S_9$, a superstructure intermediate in the series Bi_2S_3—$PbCuBiS_3$ (bismuthinite—aikinite). Acta Crystallogr. (in press).

V. Kupčik (1965), Struktur des Emplektits $CuBiS_2$. Program and Abstracts for Meeting of the Crystallographic Section of the German Mineralogical Soc., Oct. 13—16, 1965, Marburg, 16—17.

V. Kupčik und E. Makovický (1968), Die Kristallstruktur des Minerals (Pb,Ag,Bi) $Cu_4Bi_5S_{11}$. N. Jahrb. Miner., Monatsh. **1968**, 236—237.

V. Kupčik und Ludmila Veselá-Nováková (1970), Zur Kristallstruktur des Bismuthinits, Bi_2S_3. Tschermaks Miner. Petrogr. Mitt. **14**, 55—59.

E. W. Nuffield and D. C. Harris (1966), Studies of mineral sulphosalts: XX. Berryite, a new species. Canad. Mineral. **8**, 407—413.

Hajo H. Onken (1964), Manual for some computer programs for x-ray analysis. Crystallographic Laboratory, Massachusetts Institute of Technology, Cambridge, Massachusetts.

H. H. Otto und H. Strunz (1968), Zur Kristallchemie synthetischer Blei-Wismut-Spießglanze. N. Jahrb. Miner. Abh. **108**, 1—19.

Tohru Ozawa and Yoshio Takéuchi (1972), The crystal structure of $Cu_4Bi_4S_9$ and its relation to simple sulfide structures. Acta Crystallogr. A **28**, S 70 (abstract).

Linus Pauling (1960), *The nature of the chemical bond.* Third edition, Cornell University Press, Ithaca, New York.

Charles T. Prewitt (1962), Structures and crystal chemistry of wollastonite and pectolite. Ph. D. Thesis, Dept. of Geology and Geophysics, Massachusetts Institute of Technology.

G. Springer (1971), The synthetic solid-solution series Bi_2S_3—$BiCuPbS_3$ (bismuthinite—aikinite). N. Jahrb. Miner., Monatsh., 19—24.

Junkou Takagi and Yoshio Takéuchi (1972), The crystal structure of lillianite. Acta Crystallogr. B **28**, 649—651.

G. Weitz und E. Hellner (1960), Über komplex zusammengesetzte sulfidische Erze, VII. Zur Kristallstruktur des Cosalits, $Pb_2Bi_2S_5$. Z. Kristallogr. **113**, 385—402.